Inhibition of lysyl oxidase-like 2 ameliorates folic acid-induced renal tubulointerstitial fibrosis

SUNG-EUN CHOI[1], NARA JEON[2], HOON YOUNG CHOI[3,4], HYEON JOO JEONG[2,4] and BEOM JIN LIM[2,4]

[1]Department of Pathology, CHA University, CHA Bundang Medical Center, Seongnam, Kyeonggi 13496;
Departments of [2]Pathology, [3]Internal Medicine and [4]Institute of Kidney Disease Research,
Yonsei University College of Medicine, Seoul 03722, Republic of Korea

Received January 1, 2022; Accepted July 20, 2022

DOI: 10.3892/etm.2022.11585

Abstract. Tubulointerstitial fibrosis is characterized by accumulation of the extracellular matrix in the interstitium. Lysyl oxidase-like 2 (LOXL2), a member of the lysyl oxidase family, is known for promoting cancer metastasis, invasion and stromal fibrosis in various organs. Our previous study demonstrated expression of LOXL2 in kidney podocytes and tubular epithelial cells, and the association between elevated LOXL2 and tubulointerstitial fibrosis. The present study evaluated the effect of LOXL2 inhibition using an inhibitory monoclonal antibody (AB0023) on tubulointerstitial fibrosis in a folic acid-induced tubulointerstitial fibrosis mouse model. The association of LOXL2 with epithelial-mesenchymal transformation-related molecules was also evaluated *in vitro* using HK-2 cells. The present data demonstrated that AB0023 prevented the progression of tubulointerstitial fibrosis significantly, as determined by trichrome and picro-sirius red staining, as well as the total collagen assay. The mean expression of phosphorylated Smad2 and Smad4 was lower in the AB0023-treated group although it was not statistically significant. Following transforming growth factor-β (TGF-β) challenge, LOXL2-deficient HK-2 cells exhibited significantly lower expression of the mesenchymal markers vimentin and fibronectin than control HK-2 cells. In conclusion, LOXL2 inhibition ameliorates renal fibrosis through the TGF-β/Smad signalling pathway.

Introduction

As tubulointerstitial fibrosis is a common endpoint in renal disease with no effective treatment other than dialysis, the need to understand the molecules and mechanisms involved is increasingly urgent. Histologically, tubulointerstitial fibrosis is an accumulation of the extracellular matrix (ECM) in the interstitium. ECM-producing cells are primarily activated fibroblasts (1). Various cells such as pericytes, endothelial cells, residual fibroblasts and tubular epithelial cells are known to be the origin of fibroblasts (2).

The epithelial-mesenchymal transformation (EMT) has been studied in cancer and benign fibrotic diseases (3). Once acute injury is imposed on the kidney, various chemokines and growth factors cause inflammation, which in turn leads to the secretion of transforming growth factor-β (TGF-β) via release of active TGF-β from latent TGF-β-binding protein via protease cleavage (4). TGF-β is the primary molecule responsible for EMT (5,6), and the canonical and non-canonical pathways are the downstream pathways of TGF-β (4,7). The hallmark of EMT is loss of epithelial phenotypes and acquisition of mesenchymal phenotypes with activation of profibrotic genes to produce the ECM, including fibronectin and collagen types I and III (3,5,8).

Lysyl oxidase-like 2 (LOXL2) is a member of the lysyl oxidase family, originally known as a copper-dependent amine oxidase, that is involved in cross-linking collagen and elastin of the ECM (9). Studies have also demonstrated additional functions for LOXL2 independent of its catalytic activity, such as organ development (10), tumour invasion (11) and EMT (12,13).

In mice lung fibroblast cells, LOXL2 has been revealed to play prominent roles for fibrogenesis via regulation of the TGF-β/Smad signaling pathway (14). LOXL2 has been also identified to be important in promoting both glomerular and interstitial pathogenesis associated with Alport syndrome in mice (15). In a previous study conducted by the authors, it was found that LOXL2 is expressed in kidney podocytes and tubular epithelial cells, and its expression is increased in the folic acid-induced murine fibrosis model (16). In the present study, the effect and therapeutic role of LOXL2 inhibitor AB0023 on the progression of tubulointerstitial fibrosis in mice was evaluated. In order to evaluate the contribution of LOXL2 in EMT, an *in vitro* study using immortalized human proximal tubular epithelial cells (HK-2 cells) was also performed.

Materials and methods

Animal model of tubulointerstitial fibrosis and LOXL2 inhibition. Male CD1 mice at 8 weeks of age (Orient Bio,

Correspondence to: Dr Beom Jin Lim, Department of Pathology, Yonsei University College of Medicine, 50-1 Yonsei Road, Seodaemoon, Seoul 03722, Republic of Korea
E-mail: bjlim@yuhs.ac

Key words: lysyl oxidase-like 2, folic acid, tubulointerstitial fibrosis, TGF-β pathway, epithelial-mesenchymal transformation

Inc.) were used in the present study. The animals were housed in a facility maintained at 20˚C and 12-h alternating light/dark cycles with free access to rodent chow and water. Tubulointerstitial fibrosis was induced by intraperitoneal injection of folic acid (240 μg/g body weight) (17,18). The folic acid solution was prepared by dissolving folic acid powder (Sigma-Aldrich; Merck KGaA) in 0.3 M $NaHCO_3$. Control CD1 mice were injected intraperitoneally with the same volume of vehicle ($NaHCO_3$). Urinary excretion of neutrophil gelatinase-associated lipocalin (NGAL) (19) was measured immediately before injection and at 3 days after injection using a Mouse Lipocalin-2/NGAL Quantikine ELISA kit (cat. no. MLCN20; R&D Systems, Inc.) to ensure successful injection of folic acid, as manifested by a log scale increase in NGAL. The concentration of urinary NGAL was normalized by the concentration of urinary creatinine as measured by the QuantiChrom Creatinine Assay kit (BioAssay Systems). Mice without an increase in NGAL at 3 days post-folic acid injection, indicating that folic acid was not successfully injected, were omitted from the study. Ultimately, 16 mice injected with folic acid and six mice injected with vehicle were examined in the present study. The present study was approved (approval no. 2015-0247) by the Institutional Animal Care and Use Committee of the Yonsei University Health System (Seoul, Republic of Korea). All experiments involving animals were carried out in accordance with the standards set forth by the Institutional Animal Care and Use Committee of Yonsei University Health System.

To inhibit LOXL2, AB0023 (cat. no. GS-607601; Gilead Sciences, Inc.), an inhibitory monoclonal antibody against LOXL2, was used. A total of 9 of the 16 folic acid-injected mice were treated with a dosage of 15 mg/kg body weight of AB0023 at 1 week before folic acid injection and twice a week for 4 weeks afterwards. The dosage was chosen according to the manufacturer's guideline, supported by a reference study using the same intraperitoneal dosage (20). Adverse effect was not observed during the experiment. The remaining seven mice were injected with immunoglobulin G (IgG) (cat. no. GS-645864; Gilead Sciences, Inc.) at the same dosage and on the same time schedule as the AB0023 treatment group. Mice were sacrificed via cervical dislocation 4 weeks after folic acid or vehicle injection, and the right kidneys were harvested (Fig. 1). Fresh frozen tissues were stored at -70˚C for western blot analysis and collagen measurement. Additional kidney tissues were fixed in 4% formaldehyde for 24 h at room temperature and embedded in paraffin overnight at 55-65˚C using an automatic tissue processer (EFTP-FAST 360; Intelsint S.R.L.).

Evaluation of tubulointerstitial fibrosis

Semiquantitative analysis via histologic examination. Paraffin-embedded samples of the AB0023-treated, IgG-injected, and vehicle-injected groups were cut into 4-μm sections. Sections were deparaffinized by submersing slides in xylene and dehydrated in 2 changes of absolute alcohol for 2 min, 1 change of 95% alcohol for 2 min, and 1 change of 70% alcohol for 2 min. The sections were stained with Masson trichrome and picro-sirius red. For Masson trichrome, sections were treated with Weigert's iron hematoxylin for 8 min to stain nuclei, Biebrich scarlet-acid fuchsin for 15 min, phosphomolybdic-phosphotungstic acid for 15 min and aniline blue for 15 min at room temperature. For picro-sirius red staining, sections were treated with Weigert's Iron Hematoxylin for 8 min to stain nuclei and Direct Red 80 (Sigma-Aldrich; Merck KGaA) for 1 h at room temperature to visualize collagen before washing with 0.5% glacial acid. Slides were examined by light microscopy with or without polarization for picro-sirius red or trichrome staining, respectively. Images were captured serially along the cortex at x200 magnification and the area of interstitial fibrosis was measured using ImageJ software (version 1.50i; National Institutes of Health).

Quantitative analysis via total collagen analysis. The content of collagen in fresh frozen cortex was evaluated by measuring hydroxyproline using the Total Collagen Assay kit (QuickZyme Biosciences) according to the manufacturer's guide. Briefly, samples were hydrolysed at 95˚C in 6 M HCl for 20 h and then centrifuged at 13,000 x g for 10 min at room temperature. The supernatant was collected and assayed by ELISA according to the manufacturer's protocol. Total protein in the hydrolysed sample was also measured using the Total Protein Assay kit (QuickZyme Biosciences) and the relative amount of collagen per protein was analysed.

Renal cell culture and transfection. HK-2 cells were purchased from the American Type Culture Collection and cultured in Dulbecco's modified Eagle's medium/Nutrient Mixture F-12 (Gibco; Thermo Fisher Scientific, Inc.) supplemented with 10% fetal bovine serum (Gibco; Thermo Fisher Scientific, Inc.). To silence LOXL2 expression at the cellular level, LOXL2 small hairpin (sh)RNA lentiviral particles (cat. no. sc-45222-v; Santa Cruz Biotechnology, Inc.) were transduced into HK-2 cells at room temperature cultured on collagen I (2 mg/ml; cat. no. 354236; Corning Inc.,)-coated dishes (21). HK-2 cells were treated with media containing 5 μg/ml of polybrene (cat. no. sc-134220; Santa Cruz Biotechnology, Inc.), and then LOXL2 shRNA lentiviral particles and control shRNA lentiviral particles (cat. no. sc-108080; Santa Cruz Biotechnology, Inc.) of 1 and 2 multiplicity of infection (MOI) were added and incubated overnight at 37˚C. Transfected cells were selected by selection media containing 2 μg/ml puromycin dihydrochloride (cat. no. sc-108071; Santa Cruz Biotechnology, Inc.). After confirming the decrease in LOXL2 expression by reverse transcription-quantitative polymerase chain reaction (RT-qPCR) and western blot analysis, cells of 2 MOI were treated with serum-free media for 24 h and then media containing TGF-β (20 ng/ml; R&D Systems, Inc.) for 72 h. Other LOXL2-deficient cells (2 MOI) were treated with serum-free media for 24 h and then media containing vehicle (0.1% 4 mM HCl/BSA). Control shRNA lentiviral particles were transduced into another line of HK-2 cells in the same manner as that of LOXL2 shRNA particles and were further incubated with media containing either TGF-β (20 ng/ml; R&D Systems, Inc.) or vehicle (0.1% 4 mM HCl/BSA) after 24 h of serum starvation.

RT-qPCR. Total RNA of transfected cells was extracted using RNeasy kit (cat. no. 74104; Qiagen, Inc.). RNA was reverse transcribed to cDNA using the Qiagen Quantitect Reverse Transcription kit (cat. no. 205311; Qiagen, Inc.) in 20 μl reaction

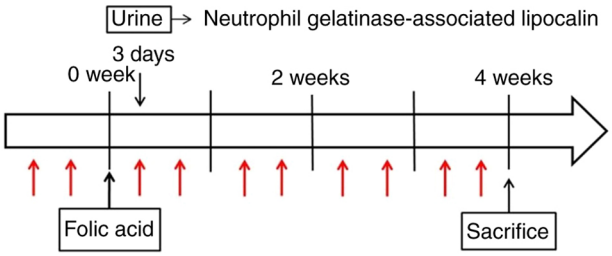

Figure 1. Injection protocol of folic acid, AB0023 (a monoclonal antibody against LOXL2), and control IgG in the CD1 mouse model. The red arrow indicates AB0023 or control IgG intraperitoneal injection (15 mg/kg). AB0023 or control IgG was injected at 4 and 1 days before folic acid injection, and twice weekly until 4 weeks after folic acid injection. Urinary neutrophil gelatinase-associated lipocalin was measured 3 days after folic acid injection to ensure successful induction of renal fibrosis.

volumes containing 1 μg of RNA. The reaction was carried out at 42˚C for 2 min, 42˚C for 15 min and held at 95˚C for 3 min. The cDNA products were diluted at 1:5 to contain 30 ng of cDNA in 3 μl for use in qPCR. qPCR was performed using a TaqMan Gene Expression Master Mix assay (cat. no. 4369016; Applied Biosystems; Thermo Fisher Scientific, Inc.), with 18S ribosomal RNA gene (cat. no. Mm03928990_g1; Applied Biosystems; Thermo Fisher Scientific, Inc.) as reference gene and human LOXL2 (cat. no. Hs00158757_m1; Applied Biosystems; Thermo Fisher Scientific, Inc.) probe according to the manufacturer's protocol. As the manufacturer does not provide the primer sequences of human LOXL2 and 18S ribosomal RNA gene, it has not been possible to provide the information. The qPCR reactions were carried out according to the product instruction (50˚C for 2 min, 95˚C for 10 min, and then 40 cycles of 95˚C for 10 sec, 60˚C 1 min). All data were analyzed using the $2^{-\Delta\Delta Cq}$ method (22).

Western blot analysis for LOXL2, Smad-related molecules and EMT-related molecules. Fresh frozen kidney tissues from mice, injected with AB0023 or control IgG followed by folic acid or injected only with vehicle, were homogenised and western blotting was performed following the same protocol as previously described by the authors (16). Radioimmunoprecipitation assay buffer (Biosesang) with a protease inhibitor cocktail (Roche Diagnostics) was prepared. The samples were centrifuged at 13,000 x g for 30 min at 4˚C. The protein concentration was measured through bicinchoninic acid protein assay kit (Thermo Fisher Scientific, Inc.) according to the manufacturer's protocol. When the protein samples (50 μg) were separated by 10% sodium dodecyl sulphate-polyacrylamide gel electrophoresis for 2 h at 100 V, they were transferred onto a polyvinylidene fluoride membrane and blocked with 3% skim milk for 1 h at room temperature. Primary antibodies were incubated with the membrane overnight at 4˚C. The anti-mouse-specific primary antibodies purchased from Cell Signaling Technology, Inc. included anti-Smad2 (1:1,000; cat. no. 5339), anti-phosphorylated (p)-Smad2 (Ser465/467; 1:500; cat. no. 3108), anti-Smad3 (1:1,000; cat. no. 9523), anti-p-Smad3 (Ser423/425; 1:1,000; cat. no. 9520) and anti-Smad4 (1:1,000; cat. no. 38454). The blocking solution used for the anti-p-Smad2 and anti-p-Smad3 antibodies contained 5% bovine serum albumin (Sigma-Aldrich; Merck KGaA). The membrane was washed with Tris-buffered saline containing 0.1% Tween-20. It was then incubated with horseradish peroxidase-labelled secondary antibodies (1:5,000; cat. no. sc-2020; Santa Cruz Biotechnology, Inc. and 1:5,000; cat. no. K4003; Dako; Agilent Technologies, Inc.) for 1 h at room temperature. Pierce Enhanced Chemiluminescence Western Blotting Substrate (Thermo Fisher Scientific, Inc.) was used to visualize protein bands. The membrane was stripped with Restore Western Blot Stripping Buffer (Thermo Fisher Scientific, Inc.) for 15 min at room temperature, and then it was incubated with an anti-β-actin antibody (1:2,000; cat. no. sc-47778; Santa Cruz Biotechnology, Inc.). The bands were semi-quantified by densitometry using ImageJ software (version 1.50i; National Institutes of Health).

In addition, HK-2 cells with LOXL2 shRNA or control transfection after TGF-β challenge or incubated with vehicle were lysed in buffer and western blotting was performed in similar manner. Due to their high molecular weight, 6%-acrylamide gel was used for fibronectin, ZO-1 and E-cadherin. Except for acrylamide percentage, all the membranes were electrophoresed under identical experimental conditions. The primary antibodies applied to HK-2 cells were anti-vimentin (1:5,000; cat. no. ab92547; Abcam), anti-E-cadherin (1:500; cat. no. 610181; BD Biosciences), anti-zonula occludens (ZO)-1 (1:500; cat. no. ab2272; Sigma-Aldrich; Merck KGaA), anti-fibronectin (1:1,000; cat. no. sc8422; Santa Cruz Biotechnology, Inc.) and anti-LOXL2 (1:500; cat. no. ab96233; Abcam).

Statistical analysis. Quantitative analysis was performed for the western blotting and RT-qPCR results. Vehicle-injected mice, folic acid-injected mice treated with AB0023, and folic acid-injected mice treated with control IgG were compared. For comparing fibrosis, Kruskal-Wallis test followed by Dunn's post hoc tests with Bonferroni corrections was performed. When comparing the folic acid injected groups treated with either AB0023 or control IgG, Mann-Whitney U test was performed. For comparing the Smads levels, Mann-Whitney U test was used. In addition, HK-2 cells with or without LOXL2 inhibition were analyzed by Kruskal-Wallis test followed by Dunn's post hoc tests with Bonferroni corrections and Mann-Whitney U test. Data are expressed as the mean ± standard deviation. The analyses were performed using SPSS version 25 software (IBM Corp.). $P<0.05$ was considered to indicate a statistically significant difference.

Results

LOXL2 inhibition prevents the progression of tubulointerstitial fibrosis in the mouse model. The amount of fibrosis measured by trichrome (Fig. 2A) and picro-sirius red staining (Fig. 2B) decreased in mice treated with AB0023, compared with the control IgG-treated group (Fig. 2C and D). Quantitative measurement of fibrosis by total collagen analysis also showed that fibrosis decreased in mice treated with AB0023 (Fig. 2E).

LOXL2 inhibition may influence the canonical TGF-β/Smad signalling pathway. Smad signaling pathway molecules, including p-Smad3, p-Smad2, and Smad4 exhibited no significant difference with LOXL2 inhibition (Fig. 3). However, the

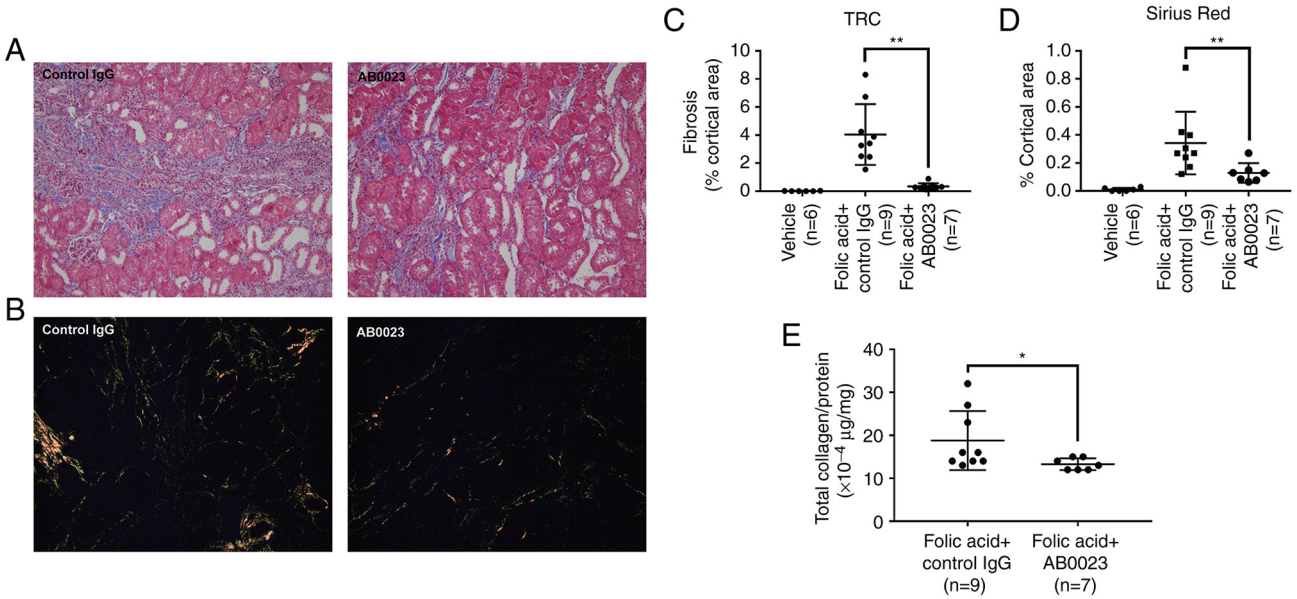

Figure 2. Effects of lysyl oxidase-like 2 inhibition on the progression of tubulointerstitial fibrosis. (A and B) Representative images of renal cortex of folic acid-injected mice treated with control IgG or AB0023. The amount of fibrosis was measured using (A and C) Masson trichrome stain and (B and D) picro-sirius red stain under polarized microscopy. The levels of fibrosis were significantly lower in the AB0023-treated group compared with the control group. (E) The total collagen assay revealed similar result. *P<0.05 and **P<0.017, resulted from Dunn's post hoc test with Bonferroni corrections.

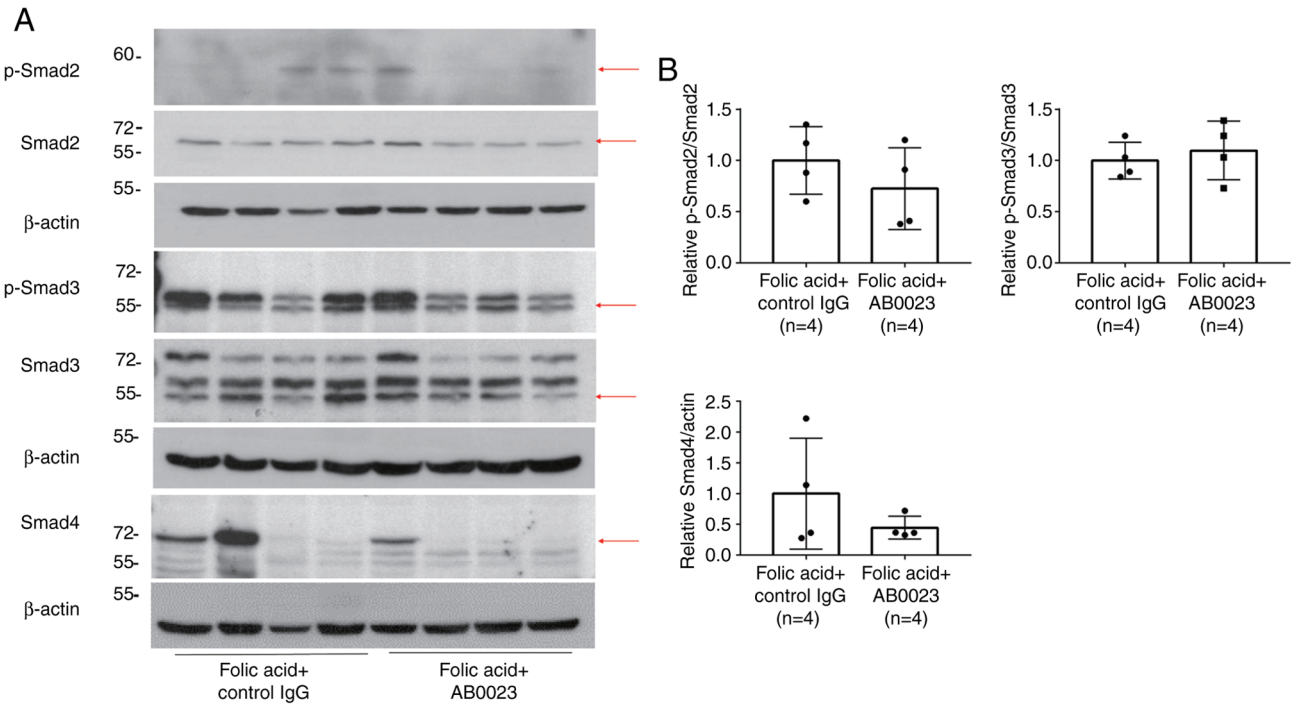

Figure 3. Effects of LOXL2 inhibition on the TGF-β/Smad pathway. (A) Western blots of p-Smad2, Smad2, p-Smad3, Smad3 and Smad4. (B) Densitometric analysis of protein bands in panel A. There was no significant difference in the level of Smad pathway-related molecules, but the amount of p-Smad2 and Smad4 tended to be lower after LOXL2 inhibition. P-values: 0.376, 0.784 and 0.010 for p-Smad2/total Smad2, p-Smad3/total Smad3 and Smad4, respectively. LOXL2, lysyl oxidase-like 2; p-, phosphorylated.

amounts of p-Smad2 and Smad4 tended to decrease in the AB0023-treated group compared with the control group.

LOXL2 knockdown in HK-2 cells reduces the expression of some EMT-associated molecules. Transfection of HK-2 cells with LOXL2 shRNA resulted in LOXL2 knockdown (Fig. S1). In control HK-2 cells transfected with control shRNA, TGF-β treatment (72 h) reduced the levels of epithelial marker E-cadherin, and increased the levels of mesenchymal markers vimentin and fibronectin. Multiple comparison analysis revealed the decreasing trends of vimentin and fibronectin level in LOXL2 knockdown cells compared with the control

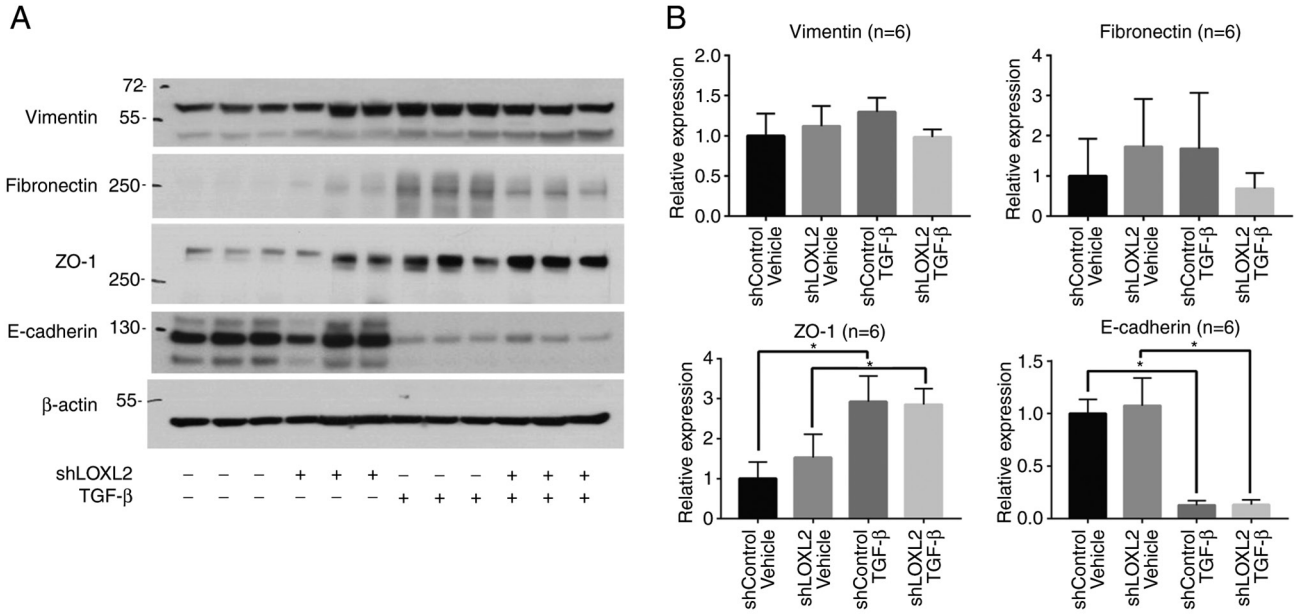

Figure 4. Expression of epithelial-mesenchymal transformation-associated molecules after TGF-β challenge in LOXL2 knockdown HK-2 cells. (A) Representative western blots of vimentin, fibronectin, ZO-1 and E-cadherin. (B) Densitometric analysis of protein bands in panel A. HK-2 cells were transfected with either control shRNA virus or LOXL2 shRNA lentivirus to knockdown LOXL2 expression. After 24 h of serum starvation, both the LOXL2-deficient cells and control cells were incubated with either TGF-β or vehicle for 72 h. Compared with control HK-2 cells, LOXL2-deficient HK-2 cells showed decreasing trend of vimentin and fibronectin expression after TGF-β challenge. *P<0.05 (n=6 for all four groups). LOXL2, lysyl oxidase-like 2; ZO-1, zonula occludens-1; sh-, small hairpin; shControl, HK-2 cells transfected with control shRNA; shLOXL2, LOXL2-deficient HK-2 cells by LOXL2 shRNA transfection.

shRNA-transduced cells after TGF-β treatment (Fig. 4). Considering that the level of vimentin and fibronectin increases after TGF-β challenge in control cells, the decreasing trend of those in LOXL2 knockdown cells after TGF-β challenge is more meaningful. The epithelial markers ZO-1 and E-cadherin did not show a significant difference after TGF-β treatment in LOXL2 knockdown and control cells, while the level of E-cadherin was markedly decreased by TGF-β challenge compared with the shControl Vehicle.

Discussion

Inhibition of LOXL2 via AB0023 has been revealed to reduce fibrosis in various organs. For instance, AB0023 attenuated postoperative fibrosis in a rabbit model of glaucoma surgery (23). AB0023 also attenuated tetrachloride-induced hepatic fibrosis in BALB/c mice, and high-dose bleomycin-induced pulmonary fibrosis in C57BL/6 mice (20). Although a clinical trial of simtuzumab, a humanized form of AB0023, resulted in no significant changes in fibrosis in human immunodeficiency virus- and hepatitis C virus-infected adults, serum samples suggested upregulation of TGF-β3 and interleukin-10 pathways with treatment, suggesting the future evaluation for clinical trials with simtuzumab after the modulation of TGF-β3 (24). It was previously observed that LOXL2 is expressed in tubular epithelial cells, and a role for LOXL2 in TGF-β-mediated tubulointerstitial fibrosis was presumed. This hypothesis is supported by the increased LOXL2 mRNA and protein levels detected in the kidneys of mice with folic acid-induced tubulointerstitial fibrosis (11). Intraperitoneal folic acid injection was used to CD1 mice model in both the previous (16) and the present study. CD1 mice were selected since it has been identified that this strain is susceptible to folic acid-induced kidney injury (25,26), and this strain showed the least mortality after folic acid injection according to our experience. The positive regulatory role of LOXL2 in tubulointerstitial fibrosis was confirmed by the reduction of fibrosis in this folic acid-induced fibrosis mouse model with the inhibition of LOXL2 by the LOXL2-specific antibody AB0023. Recently, Nguyen *et al* (27) revealed that LOXL2 inhibition leads to reduction of renal fibrosis in murine kidney injury induced by cyclosporine-A. The present study was different in two points. First, folic acid administration induces both acute kidney injury and then chronic kidney disease, a course more natural and similar to how human renal fibrosis occurs. Second, the effects of LOXL2 inhibition were examined in not only in murine models but also in HK-2 cells, a proximal tubular cell line driven from human kidney.

In addition to fibrosis, TGF-β is involved in various biological activities, such as cell proliferation, apoptosis, differentiation, autophagy and the immune response (28). Thus, it is critical to investigate therapeutic strategies related to the downstream pathways of TGF-β due to the possible adverse effects of directly targeting this cytokine (29).

EMT is a major mechanism that contributes to renal fibrosis in response to multiple molecules, including TGF-β1 (1), connective tissue growth factor (CTGF) (30), and angiotensin II (11), in tubular epithelial cells. Fibroblasts arising from tubular epithelial cells (27,31) through EMT express CTGF, a fibrogenic cytokine and a downstream mediator of the TGF-β1 pathway in renal fibrosis, although research nowadays has put more importance on resident interstitial fibroblasts (32,33). CTGF itself is also known to induce EMT in the kidney. In the kidney proximal tubule cells, TGF-β1 induces ECM proteins

such as fibronectin and collagen IV via CTGF-dependent and -independent pathways (34). Finally, the ECM turnover is imbalanced, resulting in ECM accumulation and renal fibrosis. Although the *in vivo* role of EMT has previously been questioned (35), its relationship with renal fibrosis remains to be valuable.

Among multiple molecules related to EMT, TGF-β1 is the most potent inducer of EMT (5,8). As aforementioned, EMT is a well-described process characterized by a loss of epithelial cell adhesion molecules, such as E-cadherin and ZO-1, *de novo* α-SMA expression and actin filament reorganization, transformation of myofibroblastic morphology, tubular basement membrane disruption and cell migration/infiltration into the interstitium (5,8). However, conflicting results have been reported from *in vivo* studies as tubular cells that have undergone partial EMT relay proinflammatory and profibrogenic signals to the interstitium without directly contributing to the myofibroblast population (36). Accordingly, the relationship between LOXL2 and the TGF-β pathway *in vivo,* and the TGF-β-mediated relationship between LOXL2 and EMT *in vitro*, were investigated in the present study. Thus, canonical pathway-related molecules were studied *in vivo* and markers expressed by tubular cells during EMT were studied *in vitro*.

The lack of significant differences in the level of Smad molecules after LOXL2 inhibition in the present study may be due to the lapse of time between folic acid injection and analysis. Murine kidneys were harvested at 4 weeks after this injury, by which time fibrogenesis could have already been completed. Stallons *et al* (18) reported that TGF-β1 and α-SMA levels increased until 6 days after folic acid injection, and gradually decreased afterwards in a similar experiment where a 250 mg/kg dose of folic acid was injected intraperitoneally. Tang *et al* (37) reported that after the administration of high glucose doses, the expression of p-Smad2 and p-Smad3 increased in HK-2 cells for 30 to 60 min and 30 to 120 min, respectively, before decreasing gradually. The present study differed from this experiment; in particular, the time between intervention and injury was substantially longer than that in previous studies. A more rapid analysis of Smad molecules after folic acid injection may have revealed a more pronounced change in their expression in the present study.

Although statistically less significant, the decreasing trends of the effect of AB0023 on the expression levels of pSmad2 and Smad4 are similar to those published by Wen *et al* (14), demonstrating the possible association of LOXL2 and canonical pathway. It was hypothesized that LOXL2 may act on downstream of the TGF-β pathway or LOXL2 and TGF-β may interact indirectly (14). In line with the aforementioned study, the decreasing tendency of pSmad2 and Smad4 expression after LOXL2 inhibition, reinforcing the regulatory role of LOXL2 on TGF-β/Smad signaling pathway, was also revealed in the present study. EMT is located more downstream of the TGF-β pathway than Smad molecules, and LOXL2 inhibition did not show significant difference in EMT markers other than vimentin. This possibly indicates more indirect relationship between LOXL2 and EMT compared with Smad molecules. Therefore, it was suggested that LOXL2 may be located upstream from the EMT but downstream of TGF-β, or LOXL2 may regulate the TGF-β pathway indirectly. It was found that pSmad3 level tended to increase after AB0023 treatment, whereas Wen *et al* (14) found pSmad2/3 level decreased after LOXL2 RNA inhibition. The discrepancy may be attributed to the difference in methods of LOXL2 inhibition: RNA inhibition and inhibitory antibody often has different off-targets and the power of inhibitory effect differs (38). Furthermore, the discrepancy may be attributed to the different nature of the experiment. *In vivo* experiment is complicated by various extracellular signals including cell-to-cell interaction and cell-to-ECM interaction; such unwanted effects are reduced in *in vitro* experiment.

Experiments on HK-2 cells *in vitro* after TGF-β challenge revealed no significant difference in the myofibroblast marker nor epithelial marker in LOXL2 knockdown cells. However, there was a decreasing trend in vimentin and fibronectin. These data indicated that LOXL2 may play a regulatory role in EMT. Other studies have shown no reduction in epithelial markers, such as E-cadherin, with LOXL2 inhibition after TGF-β challenge, while a significant reduction of E-cadherin was observed in the present study. However, cell types and experimental methods used in the present study differ from those previously reported (12,13,39). Although EMT markers level remained insignificant, it can be inferred that LOXL2 may be related to EMT pathway at least partially based on decreasing trends of vimentin and fibronectin. Further studies are warranted to elucidate the mechanisms underlying the LOXL2-EMT-related pathway, particularly investigating the EMT markers after blocking the TGF-β/Smad signaling pathway.

In conclusion, inhibition of LOXL2 ameliorates renal fibrosis. LOXL2 may be associated with TGF-β-mediated tubulointerstitial fibrosis and EMT. Improved understanding of the role of LOXL2 in the kidney may illuminate the pathophysiology of tubulointerstitial fibrosis and glomerulosclerosis, and potentially lead to the discovery of novel therapeutic targets for treating these conditions.

Acknowledgements

Not applicable.

Funding

The present study was supported by the Basic Science Research Program through the National Research Foundation of Korea (NRF) funded by the Ministry of Science, ICT and Future Planning (grant no. NRF-2015R1C1A1A02036671).

Availability of data and materials

All data generated or analyzed during this study are available from the corresponding author on reasonable request.

Authors' contributions

SEC performed data analysis and interpretation, drafted and revised the manuscript. NJ performed experiments and retrieved data. HYC and HJJ conceptualized the present study. BJL contributed to the conceptualization of the present study,

data analysis, interpretation of data and revising the manuscript. All authors read and approved the final version of the manuscript. SEC and BJ Lim confirm the authenticity of all the raw data.

Ethics approval and consent to participate

The present study was approved (approval no. 2015-0247) by the Institutional Animal Care and Use Committee of the Yonsei University Health System (Seoul, Republic of Korea). All experiments involving animals were carried out in accordance with the standards set forth by the Institutional Animal Care and Use Committee of Yonsei University Health System.

Patient consent for publication

Not applicable.

Competing interests

The authors declare that they have no competing interests.

References

1. Meran S and Steadman R: Fibroblasts and myofibroblasts in renal fibrosis. Int J Exp Pathol 92: 158-167, 2011.
2. Liu Y: Cellular and molecular mechanisms of renal fibrosis. Nat Rev Nephrol 7: 684-696, 2011.
3. Lamouille S, Xu J and Derynck R: Molecular mechanisms of epithelial-mesenchymal transition. Nat Rev Mol Cell Biol 15: 178-196, 2014.
4. Meng XM, Nikolic-Paterson DJ and Lan HY: TGF-β: The master regulator of fibrosis. Nat Rev Nephrol 12: 325-338, 2016.
5. Yang J and Liu Y: Dissection of key events in tubular epithelial to myofibroblast transition and its implications in renal interstitial fibrosis. Am J Pathol 159: 1465-1475, 2001.
6. Friedman SL, Sheppard D, Duffield JS and Violette S: Therapy for fibrotic diseases: Nearing the starting line. Sci Transl Med 5: 167sr161, 2013.
7. Sutariya B, Jhonsa D and Saraf MN: TGF-β: The connecting link between nephropathy and fibrosis. Immunopharmacol Immunotoxicol 38: 39-49, 2016.
8. Hills CE and Squires PE: The role of TGF-β and epithelial-to mesenchymal transition in diabetic nephropathy. Cytokine Growth Factor Rev 22: 131-139, 2011.
9. Nishioka T, Eustace A and West C: Lysyl oxidase: From basic science to future cancer treatment. Cell Struct Funct 37: 75-80, 2012.
10. Maki JM, Sormunen R, Lippo S, Kaarteenaho-Wiik R, Soininen R and Myllyharju J: Lysyl oxidase is essential for normal development and function of the respiratory system and for the integrity of elastic and collagen fibers in various tissues. Am J Pathol 167: 927-936, 2005.
11. Ahn SG, Dong SM, Oshima A, Kim WH, Lee HM, Lee SA, Kwon SH, Lee JH, Lee JM, Jeong J, *et al*: LOXL2 expression is associated with invasiveness and negatively influences survival in breast cancer patients. Breast Cancer Res Treat 141: 89-99, 2013.
12. Cuevas EP, Moreno-Bueno G, Canesin G, Santos V, Portillo F and Cano A: LOXL2 catalytically inactive mutants mediate epithelial-to-mesenchymal transition. Biol Open 3: 129-137, 2014.
13. Cuevas EP, Eraso P, Mazon MJ, Santos V, Moreno-Bueno G, Cano A and Portillo F: LOXL2 drives epithelial-mesenchymal transition via activation of IRE1-XBP1 signalling pathway. Sci Rep 7: 44988, 2017.
14. Wen X, Liu Y, Bai Y, Li M, Fu Q and Zheng Y: LOXL2, a copper-dependent monoamine oxidase, activates lung fibroblasts through the TGF-β/Smad pathway. Int J Mol Med 42: 3530-3541, 2018.
15. Cosgrove D, Dufek B, Meehan DT, Delimont D, Hartnett M, Samuelson G, Gratton MA, Phillips G, MacKenna DA and Bain G: Lysyl oxidase like-2 contributes to renal fibrosis in Col4alpha3/Alport mice. Kidney Int 94: 303-314, 2018.
16. Choi SE, Jeon N, Choi HY, Shin JI, Jeong HJ and Lim BJ: Lysyl oxidaselike 2 is expressed in kidney tissue and is associated with the progression of tubulointerstitial fibrosis. Mol Med Rep 16: 2477-2482, 2017.
17. Long DA, Woolf AS, Suda T and Yuan HT: Increased renal angiopoietin-1 expression in folic acid-induced nephrotoxicity in mice. J Am Soc Nephrol 12: 2721-2731, 2001.
18. Stallons LJ, Whitaker RM and Schnellmann RG: Suppressed mitochondrial biogenesis in folic acid-induced acute kidney injury and early fibrosis. Toxicol Lett 224: 326-332, 2014.
19. Wang W, Li Z, Chen Y, Wu H, Zhang S and Chen X: Prediction value of serum NGAL in the diagnosis and prognosis of experimental acute and chronic kidney injuries. Biomolecules 10: 981, 2020.
20. Barry-Hamilton V, Spangler R, Marshall D, McCauley S, Rodriguez HM, Oyasu M, Mikels A, Vaysberg M, Ghermazien H, Wai C, *et al*: Allosteric inhibition of lysyl oxidase-like-2 impedes the development of a pathologic microenvironment. Nat Med 16: 1009-1017, 2010.
21. Yen CL, Li YJ, Wu HH, Weng CH, Lee CC, Chen YC, Chang MY, Yen TH, Hsu HH, Hung CC, *et al*: Stimulation of transforming growth factor-beta-1 and contact with type I collagen cooperatively facilitate irreversible transdifferentiation in proximal tubular cells. Biomed J 39: 39-49, 2016.
22. Livak KJ and Schmittgen TD: Analysis of relative gene expression data using real-time quantitative PCR and the 2(-Delta Delta C(T)) method. Methods 25: 402-408, 2001.
23. Van Bergen T, Marshall D, Van de Veire S, Vandewalle E, Moons L, Herman J, Smith V and Stalmans I: The role of LOX and LOXL2 in scar formation after glaucoma surgery. Invest Ophthalmol Vis Sci 54: 5788-5796, 2013.
24. Meissner EG, McLaughlin M, Matthews L, Gharib AM, Wood BJ, Levy E, Sinkus R, Virtaneva K, Sturdevant D, Martens C, *et al*: Simtuzumab treatment of advanced liver fibrosis in HIV and HCV-infected adults: Results of a 6-month open-label safety trial. Liver Int 36: 1783-1792, 2016.
25. Fu Y, Tang C, Cai J, Chen G, Zhang D and Dong Z: Rodent models of AKI-CKD transition. Am J Physiol Renal Physiol 315: F1098-F1106, 2018.
26. Walkin L, Herrick SE, Summers A, Brenchley PE, Hoff CM, Korstanje R and Margetts PJ: The role of mouse strain differences in the susceptibility to fibrosis: A systematic review. Fibrogenesis Tissue Repair 6: 18, 2013.
27. Nguyen LT, Saad S, Shi Y, Wang R, Chou ASY, Gill A, Yao Y, Jarolimek W and Pollock CA: Lysyl oxidase inhibitors attenuate cyclosporin A-induced nephropathy in mouse. Sci Rep 11: 12437, 2021.
28. Bottinger EP and Bitzer M: TGF-beta signaling in renal disease. J Am Soc Nephrol 13: 2600-2610, 2002.
29. Pohlers D, Brenmoehl J, Loffler I, Müller CK, Leipner C, Schultze-Mosgau S, Stallmach A, Kinne RW and Wolf G: TGF-beta and fibrosis in different organs-molecular pathway imprints. Biochim Biophys Acta 1792: 746-756, 2009.
30. Cheng M, Liu F, Peng Y, Chen J, Chen G, Xiao L and Liu H: Construction of a CTGF and RFP-coexpressed renal tubular epithelial cell and its application on evaluation of CTGF-specific siRNAs on epithelial-mesenchymal transition. Urology 83: 1443. e1-e8, 2014.
31. Vadasz Z, Kessler O, Akiri G, Gengrinovitch S, Kagan HM, Baruch Y, Izhak OB and Neufeld G: Abnormal deposition of collagen around hepatocytes in Wilson's disease is associated with hepatocyte specific expression of lysyl oxidase and lysyl oxidase like protein-2. J Hepatol 43: 499-507, 2005.
32. Burns WC, Twigg SM, Forbes JM, Pete J, Tikellis C, Thallas-Bonke V, Thomas MC, Cooper ME and Kantharidis P: Connective tissue growth factor plays an important role in advanced glycation end product-induced tubular epithelial-to-mesenchymal transition: Implications for diabetic renal disease. J Am Soc Nephrol 17: 2484-2494, 2006.
33. Mack M and Yanagita M: Origin of myofibroblasts and cellular events triggering fibrosis. Kidney Int 87: 297-307, 2015.
34. Qi W, Chen X, Poronnik P and Pollock CA: Transforming growth factor-beta/connective tissue growth factor axis in the kidney. Int J Biochem Cell Biol 40: 9-13, 2008.
35. Kriz W, Kaissling B and Le Hir M: Epithelial-mesenchymal transition (EMT) in kidney fibrosis: fact or fantasy? J Clin Invest 121: 468-474, 2011.

36. Grande MT, Sanchez-Laorden B, Lopez-Blau C, De Frutos CA, Boutet A, Arévalo M, Rowe RG, Weiss SJ, López-Novoa JM and Nieto MA: Snail1-induced partial epithelial-to-mesenchymal transition drives renal fibrosis in mice and can be targeted to reverse established disease. Nat Med 21: 989-997, 2015.
37. Tang WB, Ling GH, Sun L, Zhang K, Zhu X, Zhou X and Liu FU: Smad anchor for receptor activation regulates high glucose-induced EMT via modulation of Smad2 and Smad3 activities in renal tubular epithelial cells. Nephron 130: 213-220, 2015.
38. Weiss WA, Taylor SS and Shokat KM: Recognizing and exploiting differences between RNAi and small-molecule inhibitors. Nat Chem Biol 3: 739-744, 2007.
39. Peinado H, Cruz MDC, Olmeda D, Csiszar K, Fong KSK, Vega S, Nieto MA, Cano A and Portillo F: A molecular role for lysyl oxidase-like 2 enzyme in snail regulation and tumor progression. EMBO J 24: 3446-3458, 2005.